LETTERS
PUBLISHED ONLINE: 19 SEPTEMBER 2010 | DOI: 10.1038/NMAT2853
nature materials

Molecular manipulator driven by spatial variation of liquid-crystalline order

Sadaki Samitsu*†, Yoichi Takanishi and Jun Yamamoto*

Collective long-range interactions between micrometre-sized impurities in liquid crystals result from the elastic distortion of the liquid-crystalline order[1–8]. For substantially smaller polymeric impurities, what is relevant is not the elastic interaction between them but the coupling between the scalar nematic order parameter S and the polymer concentration ϕ. This coupling originates from local molecular interactions, but becomes long ranged because the total polymer concentration is conserved over the whole sample. Here, we propose a new mechanism by which the spatial variation of S generates a force, mediated by the coupling between S and ϕ, that transports nanoscale polymeric impurities. We have designed a prototype of a molecular manipulator that moves molecules along spatial variations of the scalar order parameter, modulated in a controlled manner by spot illumination of an azobenzene-doped nematic phase with ultraviolet light. We also demonstrate the use of the manipulator for the measurement of the anisotropic diffusion constant of a polymer in the nematic phase. The manipulator can control the spatial variation of the polymer concentration, thus showing promise for use in the design of hybrid soft materials.

Impurity-induced frustration in liquid-crystalline systems can lead to the development of hierarchical structures with dimensions ranging from nanometres to micrometres, and transport of molecules. Simple model systems with liquid-crystalline order of nematic type containing micrometre-scale colloidal impurities have been well studied[1–8], cause and revealed that the collective long-range interactions mediated by the liquid-crystalline director field drive the directional motion of the colloids[1–4] and can result in the appearance of one- and two-dimensional periodic structures[5–8].

Although many studies have investigated the impurity-induced director-field distortion, the coupling between the scalar nematic order parameter S and the impurity concentration ϕ has not been sufficiently investigated[9]. This is probably because the distortion caused by impurities with size much larger than the length of the liquid-crystal molecules is of such large scale that it does not influence S (ref. 10). On the other hand, the director-field distortion linearly increases with decreasing impurity size. The distortion disappears for very small (nanoscale) inclusions because the anchoring conditions become relatively weak owing to the large energetic loss of the elastic distortion of the director field[11]. It is in fact questionable whether continuum elasticity theory can be used to describe the interactions between liquid crystals and nanoscale inclusions.

A nanoscale impurity such as a flexible polymer molecule thus does not induce elastic distortion of the director field, but it disturbs the local liquid-crystalline order and thereby effectively couples with S. The order parameter is reduced by the presence of the polymer, increasing the free energy of the system[12]. A beautiful demonstration was given in the discovery of the polymer-stabilized blue phase[13]. Considering the great number of disclination lines (that is, spontaneous defects) in cholesteric blue phases, they conjectured that flexible non-mesogenic polymers introduced into the blue phase concentrate in the disclination core—the core is in an isotropic state and the disordered polymer is more miscible with an isotropic phase than with the ordered liquid-crystal phase. In an analogous reasoning, we predict the existence of a direct coupling between S and polymer concentration ϕ that is independent of the distortion of the director field ($\mathrm{d}\boldsymbol{n}/\mathrm{d}\boldsymbol{x}$). We propose and demonstrate a molecular manipulator, the operation of which is based on this coupling; the manipulator concentrates polymer molecules in one part of the sample by acting on the local value of the nematic order parameter.

Spatial variations in the scalar order parameter can be induced in a controlled manner by the *trans–cis* isomerization of azobenzene when excited by ultraviolet irradiation[14]; whereas the linear *trans*-azobenzene blends in with the host nematic phase, the bent shape acquired by the molecules in their excited *cis*-state disturbs the liquid-crystalline order, inducing a local decrease in S in the area of irradiation. The principle of operation of the proposed manipulator is different from that of conventional optical tweezers[15] in that the manipulation force described here is mediated by the coupling between S and ϕ.

We use local illumination with unpolarized ultraviolet light to modulate $S(x)$ of a nematic phase containing azobenzene mesogens, verifying the spatial variation of S by measuring the optical birefringence $n_a(x,y) = n_{\parallel} - n_{\perp}$. Details of the measurements are described in the Methods section and in Supplementary Fig. S1. The interference colour is uniform before ultraviolet irradiation, indicating that n_a is constant throughout the sample. As n_a is proportional to S (ref. 16), this implies that S is also spatially homogeneous. When the sample is irradiated by ultraviolet light, the interference colour in the irradiated area changes rapidly, as shown in Fig. 1a. Profiles of the spatially modulated $n_a(x,y)$ are obtained along two cross-sections, parallel and perpendicular to the director, by rotating the spectrometer. The measured birefringence n_a, and thus S, decreases by about 20% in the illuminated area. It should be noted that neither isotropic/nematic phase boundaries nor defect patterns are observed during the irradiation.

We then study the manipulation of a model fluorescent polymer. We can monitor the spatial variation of the polymer concentration by observing the intensity of its two-dimensional fluorescence image (Fig. 1b,c). The vertical axis labelled δA is

Division of Physics and Astronomy, Graduate School of Science, Kyoto University, Kitashirakawa-Oiwakecho, Sakyo-ku, Kyoto 606-8502, Japan. †Present address: Functional Thin Films Group, Organic Nanomaterials Center, National Institute of Materials Science, 1-1 Namiki, Tsukuba 305-0044, Japan.
*e-mail: SAMITSU.Sadaki@nims.go.jp; junyama@scphys.kyoto-u.ac.jp.

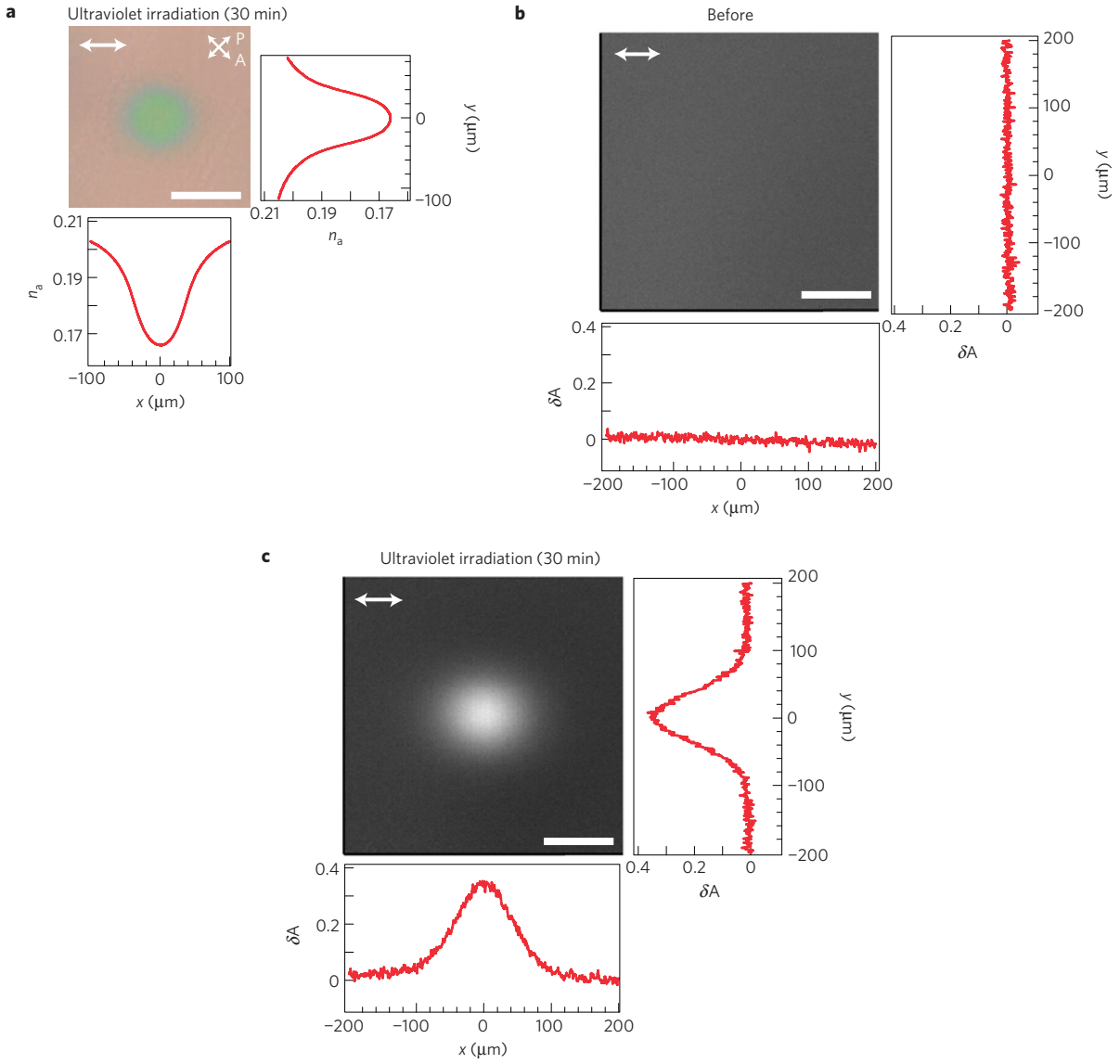

Figure 1 | Spatial variation of the scalar order parameter and the excess polymer concentration before and after ultraviolet irradiation. a, Polarizing microscope image obtained by irradiating the centre of the imaging area with patterned ultraviolet light for 30 min. The polarizer and analyser (thin white arrows) were tilted relative to the rubbing direction (bold white arrow) by about ±45° and were in a crossed configuration. The optical birefringence profile of the sample, $n_a(x,y)$, was determined using data from the imaging spectrometer (details in Supplementary Fig. S1). A large decrease in the birefringence was observed in the ultraviolet-irradiated region. **b**,**c**, Fluorescence images and cross-sections of the sample before (**b**) and after (**c**) ultraviolet irradiation. Fluorescence intensity profiles are determined along cross-sections parallel and perpendicular to the director. Before ultraviolet irradiation, the fluorescence intensity was spatially uniform. After ultraviolet irradiation, the fluorescence intensity at the centre of the image increased, clearly indicating the accumulation of the fluorescent polymer. The white scale bar corresponds to 100 μm.

the excess fluorescence intensity defined as $A/A_0 - 1$, where A_0 is the fluorescence intensity of the image in the initial state. Before ultraviolet irradiation, the polymer concentration is uniform throughout the sample (Fig. 1b); after irradiating for 30 min, the fluorescence intensity increases significantly in the irradiated area (Fig. 1c). Assuming that the fluorescence intensity is proportional to the polymer concentration (see below), the increase in the latter is estimated to be about 35% in the irradiated area. This observation, together with the modulation of $S(x)$ demonstrated above, proves that the spatial variation of the scalar order parameter drives the transport of polymer molecules, and that the developed prototype can concentrate the polymer in a desired location.

Figure 2a shows that the excess fluorescence intensity δA at the centre of the irradiated area is almost proportional to the excess birefringence δn_a ($\delta n_a = n_a/n_{a0} - 1$). Here, the subscript 0 denotes the value in the initial state (that is, the state before ultraviolet irradiation). We assume the following linear relationships: the excess concentration $\delta\phi$ ($= \phi/\phi_0 - 1$) is proportional to δA, and the change in the scalar order parameter, $\delta S(= S - S_0)$, varies linearly with δn_a. Thus, it can be concluded that $\delta\phi$ is almost proportional to $-\delta S$. A comparison of Fig. 1a and c confirms that the spatial polymer concentration profile agrees with $S(x)$. As $-\delta n_a$ is almost proportional to the square root of the ultraviolet intensity (Supplementary Fig. S2), we can vary the polymer concentration in a controlled manner by varying the spatial distribution of the ultraviolet-light intensity.

Figure 2b shows the time evolution of δA after ultraviolet irradiation. The inset shows the variation in n_a at the centre of the irradiated area. The response time of δA is about 15 min, which is much longer than that of the decrease in n_a (~ 25 s). The time

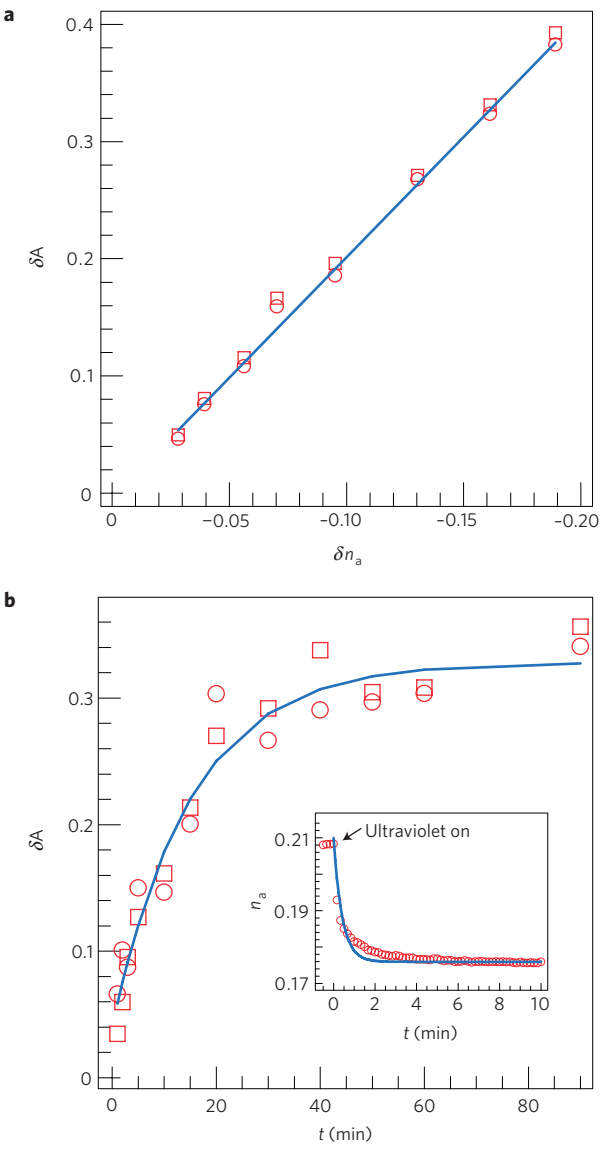

Figure 2 | Excess birefringence δn_a and ultraviolet-irradiation time dependencies of the excess fluorescence intensity δA. a, Excess fluorescence intensity δA as a function of the excess birefringence δn_a. Ultraviolet light was radiated for 30 min at 60 °C. δA increases almost linearly with $-\delta n_a$. **b**, δA as a function of the ultraviolet-irradiation time. The δA values were calculated from the cross-sections in the fluorescence image that were parallel (circles) and perpendicular (squares) to the director. The blue line indicates the exponential increase of δA with time; response time ~15 min. δA attains a saturation level when the osmotic pressure of the excess polymers is balanced by the reduced chemical potential, which can be derived from the free energy of the nematic phase. The time evolution of n_a at 600 nm during ultraviolet irradiation is shown in the inset; response time ~25 s.

taken for manipulation, τ, can be shortened by decreasing the size of the irradiated area. On the other hand, the spatial resolution of the manipulator is estimated to be about 10 μm, and it is limited by the broadening of the edge of the irradiation pattern, which is due to the thermal diffusion of the low-molecular-weight azobenzene. However, the resolution could be improved by using high-molecular-weight azobenzenes or an azobenzene-containing polymer network.

To corroborate the proposed mechanism for the function of the molecular manipulator, we now discuss other factors that might induce a spatial variation in the polymer concentration. The first factor is temperature gradients, which can drive the transport of molecules (thermal diffusion or Soret effect)[17]. However, temperature gradients can be ignored in this study because the photoisomerization of azobenzene is an isothermal process[14]. Using a 15-μm-diameter thermocouple, we directly measured the temperature of the ultraviolet-illuminated region with the same power as when using the molecular manipulator. As expected, we did not find any local temperature increase within experimental accuracy (±0.2 °C). Furthermore, as discussed below (see also Table 1), when the whole sample was heated to a temperature where it transformed to the isotropic liquid phase, no polymer was accumulated on ultraviolet irradiation. This observation rules out the relevance of temperature gradients and heat flow in affecting the spatial variation of the polymer concentration.

Another factor that should be considered is the possibility of director reorientation caused by the intense irradiation with a polarized laser beam[4]. We measured the director orientation before and after ultraviolet-light irradiation, confirming that the director was orientated in the rubbing direction even after ultraviolet-light irradiation (Supplementary Fig. S3). Finally, if a macroscopic isotropic/nematic interface appears in the sample, strong long-range interaction between the interface and impurities can be induced. In particular, a charged impurity can be subjected to a flexoelectric polarization effect[9]. We were careful to maintain low enough ultraviolet-irradiation intensity that the sample did not undergo the transition to the isotropic phase anywhere, an effect that would have introduced an isotropic/nematic phase boundary. Furthermore, the polymer used in the present system is electrically neutral (Supplementary Fig. S4). Figure 1c clearly shows that in the final steady state, the polymers accumulated at the centre of the ultraviolet-irradiated area and not at the edge; that is, the excess polymer concentration invariably depends on the local value of the scalar order parameter (lower S leading to higher ϕ), not on the spatial gradient dS/dx. In addition, the polymer concentration profile did not show any angular dependence. Thus, the possibility that other anisotropic effects such as director-field distortion and flexoelectric polarization influence the polymer accumulation can be ruled out.

Summarizing, we can identify three requirements to induce an appropriate spatial variation in the scalar order parameter for producing the desired manipulation force: a nematic phase, azobenzene doping and ultraviolet light. Without any one of these, the molecular manipulator cannot function because the scalar order parameter becomes spatially constant. We experimentally show the necessity of these three requirements (Table 1) for the operation of the molecular manipulator, on the basis of the coupling between S and ϕ for the liquid crystals 7CB (4-*n*-heptyl-4'-cyanobiphenyl) and E44. In essence, an osmotic pressure generated by the accumulation of polymer at one location should be balanced by a reduction in the chemical potential of the polymer in the same location. This can be determined from the change in free energy of the nematic phase corresponding to the ultraviolet-induced local decrease in the scalar order parameter. The spatial variation of the scalar order parameter can be precisely controlled by the *trans–cis* isomerization of azobenzene molecules excited by spot illumination with ultraviolet light (Supplementary Fig. S2).

Supplementary Fig. S5 shows the process of transient accumulation of the polymer for illumination through a small iris (Supplementary Fig. S5(a1–e1)) and a large iris (Supplementary Fig. S5(a2–e2)). In the early stages of the accumulation process, the concentration of the polymer transiently increases at the edge of the irradiated area, as evident in Supplementary Fig. S5(c2), because the flux of the polymer is proportional to the spatial gradient of the scalar order parameter (dS/dx). However, the concentration profile in the final steady state completely follows the spatial variation of

Table 1 | Experimental verification of the three parameters required for the manipulation of polymers.

Host nematic liquid crystal	Parameter i Phase	Parameter ii Concentration of azobenzene (wt%)	Parameter iii Radiation	δS	Manipulation
E44	Nematic	4	Ultraviolet	<0	Accumulated
7CB	*Isotropic*	4	Ultraviolet	0	Not accumulated
E44	Nematic	*0*	Ultraviolet	0	Not accumulated
E44	Nematic	4	*Visible*	0	Not accumulated

The wavelength of the ultraviolet light was ~350 nm; the wavelength of the visible light was ~500 nm. The manipulator works (polymers accumulate) only when all three criteria are met.

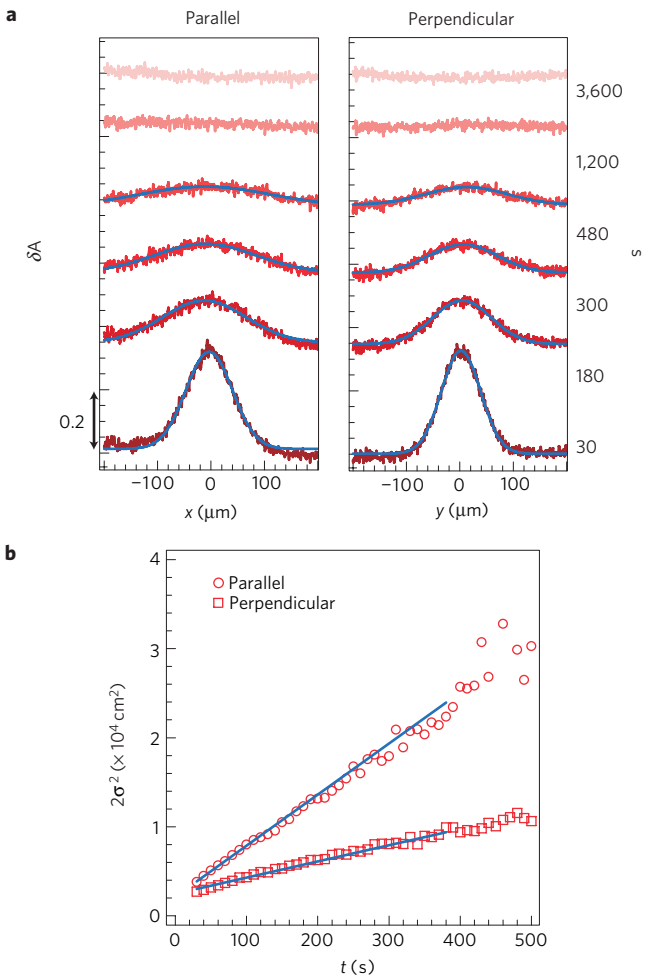

Figure 3 | Anisotropic diffusion of accumulated polymers in the nematic phase after switching off the ultraviolet irradiation. a, Decrease in δA determined using the cross-sections in the fluorescence images after irradiation with visible light; cross-sections parallel (left) and perpendicular (right) to the director were considered. The time instants at which the decreases were calculated were 30, 180, 300, 480, 1,200 and 3,600 s. The blue lines indicate the Gaussian fits to the data points. **b**, Standard deviations ($2\sigma^2$) obtained from the Gaussian fits plotted as a function of the time elapsed after the removal of the spatial variation of the scalar order parameter. The slopes of linear fits to the standard deviations obtained from the cross-sections parallel (circles) and perpendicular (squares) to the director give the anisotropic diffusion constants D for the respective directions.

the value of the scalar order parameter, which closely corresponds to the profile of δn_a; this is evident from a comparison between Supplementary Fig. S5(b1) and (e1) and between Supplementary Fig. S5(b2) and (e2).

The excess concentration of the polymer in the ultraviolet-irradiated area must be compensated by a reduction in the amount of polymer in the surrounding non-irradiated area so that the total polymer concentration is conserved. A consequence of the conservation law is that local molecular interactions between polymer and liquid-crystal molecules exhibit long-range features. It should be noted that the coupling constant α in a term describing the coupling between S and ϕ in a free-energy formula represents all local interactions between polymer molecules and liquid-crystal molecules. Its sign can be either positive or negative, the former implying that the polymer disturbs the liquid-crystalline order, and hence it corresponds to accumulation of polymer at locations of low S. On the other hand, we have experimentally found that some solute molecules such as α-quaterthiophene show negative α, meaning that these solutes are expelled from the irradiated region. Thus, when the molecular manipulator operates, the sign of α determines the direction of motion of solute polymers. As the sign of α is characteristic of the solute species, when the nematic phase contains several types of solute we can control the directional transport and concentration variation of each solute individually. Detailed results in the case of negative α will be presented in the near future.

The polymer molecules accumulated in the ultraviolet-irradiated area can be released by illuminating the sample with visible light, inducing the reverse azobenzene isomerization to the *trans* state, thus quickly removing the spatial variation of S. This leads to diffusive redispersion of the polymer molecules throughout the sample. In the nematic phase, we can detect the anisotropic diffusion of the polymer molecules by analysing the time evolution of the fluorescence profile during the diffusion. In comparison with the conventional optical methods used for measuring the diffusion constant of a solute, a remarkable feature of our method is that the diffusion is driven by the real osmotic pressure resulting from spatial polymer concentration differences. As the manipulation force can be controlled by varying the intensity of the ultraviolet light and the size and shape of the irradiated spot, we can accurately control the initial value of $\delta\phi$. We record time-lapse fluorescence images and analyse the image cross-sections in directions parallel and perpendicular to the director after the visible-light irradiation of the sample (Fig. 3a). The ultraviolet-light spot is circular; therefore, the spatial variation of $\delta\phi$ should be modulated without any angular dependence in the initial state. On the other hand, the anisotropy of the diffusion constant induces anisotropic spatial variation of $\delta\phi$ transiently as evident in Fig. 3. The standard deviations of the cross-sections obtained from Gaussian fits, $2\sigma^2$, increase almost linearly with the elapsed time (Fig. 3b). Owing to the small thickness of the sample cell (about 10 μm), the diffusion process is well explained by a two-dimensional random-diffusion model involving anisotropic diffusion constants[18]. The linear relation between the standard deviations and the elapsed time is determined for both cross-sections, and the slopes of the linear fits give the respective diffusion constants, that is, $2\sigma_{\parallel,\perp}{}^2 \propto 4D_{\parallel,\perp}t$. Thus, the diffusion constants for directions parallel

and perpendicular to the director, $D_{\parallel}$ and $D_{\perp}$, are determined to be 1.4×10^{-7} and 4.6×10^{-8} cm^2 s^{-1}, respectively. $D_{\parallel}$ is nearly three times $D_{\perp}$, which is qualitatively consistent with the observations of previous studies employing other techniques[19–21].

Methods

An azobenzene liquid crystal (3.5 or 4.0 wt%) was added to a nematic liquid-crystal mixture (E44; Merck). The mixture was doped with a small amount of a fluorescent polymer (0.01 wt%) to introduce molecular impurities. The chemical structures of the azobenzene molecule and the fluorescent polymer are shown in Supplementary Fig. S4. The ternary mixture was introduced by capillary action into a sample cell that was at a temperature above the clearing temperature of the mixture and then slowly cooled to the nematic phase to ensure that the director showed a planar homogeneous alignment. The sample cell (E.H.C.) used in this study consisted of two glass slides coated with rubbed polyimide layers and separated by 10 μm.

Polarizing and fluorescence microscopy were carried out using an Olympus polarizing microscope, BX-51P, equipped with a 100 W mercury lamp and a temperature controller. The sample temperature was maintained at 60 °C. An isothermal, reversible and well-controlled spatial variation in the scalar order parameter was induced by a photo-induced *trans*-to-*cis* conformational change of the azobenzene component in the nematic liquid-crystal mixture. The azobenzene concentration was kept low (<4 wt%) such that the isomerization would only modulate S, not induce a phase transition to the isotropic phase[14]. This was further ensured by keeping the intensity of the ultraviolet light low ($I < 16$ mW cm^{-2}). Using a fluorescence mirror unit (U-MWU2, Olympus), unpolarized ultraviolet light (wavelength λ: 300–400 nm) was passed through a small iris and an objective lens (×50) to illuminate the sample locally. The diameter of the illuminated area on the sample was about 80 μm. Whereas polarized laser radiation leads to frequent changes in the orientation of the nematic director[14], unpolarized ultraviolet radiation does not cause the orientation of the director to change (Supplementary Fig. S3), but changes the scalar order parameter owing to its effect on the azobenzene conformation (Fig. 1a). After ultraviolet irradiation, using a fluorescence mirror unit (U-MWBV2, Olympus), we irradiated the whole imaging area with visible light (λ: 400–450 nm) to quickly remove the spatial variation of the scalar order parameter. The spatial modulation of the optical birefringence disappeared within 10 s. Fluorescence images were then recorded without a polarizer by using a fluorescence mirror unit (U-MWIB3, Olympus) and a Hamamatsu Photonics system comprising a chilled CCD (charge-coupled device) camera (C5985H), a CCD camera driver (C6391) and an image processor (ARGUS). The fluorescence intensity A was normalized by the intensity of the initial fluorescence A_0 from the fluorescent polymer when it was homogeneously distributed throughout the sample.

Received 20 April 2009; accepted 11 August 2010; published online 19 September 2010

References

1. Poulin, P., Stark, H., Lubensky, T. C. & Weitz, D. A. Novel colloidal interactions in anisotropic fluids. *Science* **275,** 1770–1773 (1997).
2. Ruhwandl, R. W. & Terentjev, E. M. Long-range forces and aggregation of colloidal particles in a nematic liquid crystal. *Phys. Rev. E* **55,** 2958–2961 (1997).
3. Yoda, M., Yamamoto, J. & Yokoyama, H. Direct observation of anisotropic interparticle forces in nematic colloids with optical tweezers. *Phys. Rev. Lett.* **92,** 185501–185501 (2004).
4. Muševič, I. *et al.* Laser trapping of small colloidal particles in a nematic liquid crystal: Clouds and ghosts. *Phys. Rev. Lett.* **93,** 187801–187801 (2004).
5. Loudet, J. C., Barois, P. & Poulin, P. Colloidal ordering from phase separation in a liquid-crystalline continuous phase. *Nature* **407,** 611–613 (2000).
6. Yamamoto, J. & Tanaka, H. Transparent nematic phase in a liquid-crystal-based microemulsion. *Nature* **409,** 321–324 (2001).
7. Smalyukh, I. I., Lavrentovich, O. D., Kuzmin, A. N., Kachynski, A. V. & Prasad, P. N. Elasticity-mediated self-organization and colloidal interactions of solid spheres with tangential anchoring in a nematic liquid crystal. *Phys. Rev. Lett.* **95,** 157801–157801 (2005).
8. Muševič, I., Škarabot, M., Tkalec, U., Ravnik, M. & Žumer, S. Two-dimensional nematic colloidal crystals self-assembled by topological defects. *Science* **313,** 954–958 (2006).
9. Tatarkova, S. A., Burnham, D. R., Kirby, A. K., Love, G. D. & Terentjev, E. M. Colloidal interactions and transport in nematic liquid crystals. *Phys. Rev. Lett.* **98,** 157801–157801 (2007).
10. Kleman, M. & Lavrentovich, O. D. *Soft Matter Physics: An Introduction* (Springer-Verlag, 2003).
11. Anderson, V. J., Terentjev, E. M., Meeker, S. P., Crain, J. & Poon, W. C. K. Cellular solid behaviour of liquid crystal colloids. 1. Phase separation and morphology. *Eur. Phys. J. E* **4,** 11–20 (2001).
12. Matsuyama, A. & Kato, T. Phase separations and orientational ordering of polymers in liquid crystal solvents. *Phys. Rev. E* **59,** 763–770 (1999).
13. Kikuchi, H., Yokota, M., Hisakado, Y., Yang, H. & Kajiyama, T. Polymer-stabilized liquid crystal blue phases. *Nature Mater.* **1,** 64–68 (2002).
14. Ikeda, T. Photomodulation of liquid crystal orientations for photonic applications. *J. Mater. Chem.* **13,** 2037–2057 (2003).
15. Grier, D. G. A revolution in optical manipulation. *Nature* **424,** 21–27 (2003).
16. Takanishi, Y., Yoshimoto, M., Ishikawa, K. & Takezoe, H. Development of the nematic liquid crystal compounds derived from phenyl acetylene group with large birefringence. *Mol. Cryst. Liq. Cryst.* **331,** 619–625 (1999).
17. Duhr, S. & Braun, D. Why molecules move along a temperature gradient. *Proc. Natl Acad. Soc.* **103,** 19678–19682 (2006).
18. Tyrrell, H. J. V. & Harris, K. R. *Diffusion in Liquids: A Theoretical and Experimental Study* (Butterworth, 1984).
19. Hara, M., Ichikawa, S., Takezoe, H. & Fukuda, A. Binary mass diffusion constants in nematic liquid crystals studied by forced Rayleigh scattering. *Jpn. J. Appl. Phys.* **23,** 1420–1425 (1986).
20. Etchegoin, P. Fluorescence photobleaching recovery spectroscopy in a dye doped nematic liquid crystal. *Phys. Rev. E* **59,** 1860–1867 (1999).
21. Link, S., Chang, W-S., Yethiraj, A. & Barbara, P. F. Anisotropic diffusion of elongated and aligned polymer chains in a nematic solvent. *J. Phys. Chem. B* **110,** 19799–19803 (2006).

Acknowledgements

The authors are very grateful to S. Ujiie for providing the azobenzene derivatives and to J. Lagerwall for his kind proofreading and helpful comments on this manuscript. This work was partly supported by a Grant-in-Aid for Scientific Research on Priority Area 'Non-equilibrium soft matter physics', a Grant-in-Aid for Scientific Research (A) (No. 18204037), a Grant-in-Aid for Young Scientists (B) (No. 21740312), a Grant-in-Aid for the Global COE Program 'The Next Generation of Physics, Spun from Universality and Emergence' from the Ministry of Education, Culture, Sports, Science and Technology (MEXT) of Japan, the Toray Science Foundation and the Murata Science Foundation.

Author contributions

J.Y. conceived the initial idea. S.S. designed and conducted the experiments and analysed the results. Y.T. advised on the experiments. All authors discussed the results and implications, and wrote and commented on the manuscript at all stages.

Additional information

The authors declare no competing financial interests. Supplementary information accompanies this paper on www.nature.com/naturematerials. Reprints and permissions information is available online at http://npg.nature.com/reprintsandpermissions. Correspondence and requests for materials should be addressed to S.S. or J.Y.